Chapter 7. $[Mo(CO)_4(N\text{-}N)]$ Laboratory Results and Discussion

A series of $[Mo(CO)_4(N\text{-}N)]$ complexes to be used in an integrated laboratory experiment were investigated before introduction into the undergraduate curriculum. As students are permitted to use any N-N ligands they wish in their experiments, this is not a comprehensive review of all $[Mo(CO)_4(N\text{-}N)]$ systems that have been investigated for this project. Table 6.1 (pg 65) lists the compounds that were synthesized and characterized. The preparation of the series of $[Mo(CO)_4(N\text{-}N)]$ complexes was adapted from a literature synthesis of $[Mo(CO)_4(bpy)]$.[79,96] With the exception of $[Mo(CO)_4(5\text{-}Cl\text{-}1,10\text{-}phen)]$ and $[Mo(CO)_4(5\text{-}nitro\text{-}1,10\text{-}phen)]$, each of these complexes can be synthesized both thermally and photolytically from $[Mo(CO)_6]$ + N-N, Scheme 7.1.

Scheme 7.1. Photolytic Synthetic Scheme (A) and Thermal Synthetic Scheme (B) for $[Mo(CO)_4(bpy)]$, where bpy = 2,2'-Bipyridine.

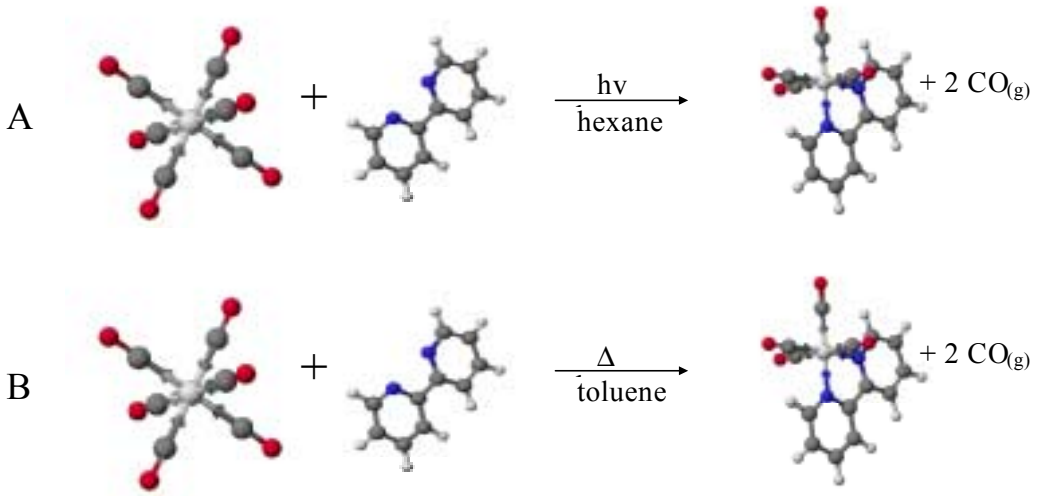

Atom Types: blue = nitrogen, gray = carbon, white = hydrogen, red = oxygen.

The electrochemical properties of the series of $[Mo(CO)_4(N\text{-}N)]$ systems were investigated (Table 7.1 and Figures 7.1-7.9). Cyclic voltammograms for the $[Mo(CO)_4(N\text{-}N)]$ systems are described by $Mo^{0/+}$ oxidations and ligand reductions, with the exception of the complexes where N-N = DPA, ethylenediamine, and TMEDA.[98] These three $[Mo(CO)_4(N\text{-}N)]$ complexes do not display ligand reductions. The $Mo^{0/+}$ oxidations are irreversible; therefore oxidation potentials are reported as $E_p^{\ a}$ ($E_{peak}^{\ anodic}$) rather than an $E_{1/2}$ values. The $N\text{-}N^{0/-}$ reductions are reversible. Reduction potentials are therefore reported as $E_{1/2}$.

Table 7.1. Cyclic Voltammetric Data for $[Mo(CO)_4(N\text{-}N)]$ Systems.[a]

(N-N)	$E_p^{\ anodic\ (b)}$ (mV)	$E_{1/2}^{\ b}$ (mV)
1,10-phen	690	-1520
5-chloro-1,10-phen	710	-1400
5-nitro-1,10-phen	740	-640
4,7-Me_2-1,10-phen		
4,7-Ph_2-1,10-phen	700	-1430
bpy	830	-1520
4,4'-Me_2-bpy	760	-1620
DPA	820	na
en	700	na
TMEDA	700	na

[a]Measurements taken in CH_3CN with 0.1 M Bu_4PF_6 supporting electrolyte, 200 mv/s scan rate. [b]Potentials reported versus Ag/AgCl reference electrode (0.29 V vs. NHE, 0.44 V vs. $Cp_2Fe^{0/+1}$).[69]

The cyclic voltammetric data of $[Mo(CO)_4(N\text{-}N)]$ complexes provides information pertaining to the relative orbital energies of the metal and N-N ligand based orbitals. As the electron withdrawing character of the N-N ligand increased, the $Mo^{0/+}$ oxidation shifts to more positive potential (harder to oxidize), and the $N\text{-}N^{0/-}$ reduction shifts to more positive potential (easier to reduce); the reductive electrochemistry exhibits a much larger shift than the oxidative electrochemistry. The cyclic voltammograms for the $[Mo(CO)_4(bpy)]$, $[Mo(CO)_4(1,10\text{-phen})]$, $[Mo(CO)_4(5\text{-nitro-}1,10\text{-phen})]$, and $[Mo(CO)_4(4,7\text{-}Ph_2\text{-}1,10\text{-phen})]$ complexes (Figures 7.1 - 7.3 and 7.6) show clean reversible reduction couples for the ligands, and irreversible $Mo^{0/+}$ oxidations. $[Mo(CO)_4(5\text{-nitro-}1,10\text{-phen})]$ exhibits a second reductive couple at –0.84 V. This is the reduction of the 5-nitro substitutent on the N-N ligand.

The complexes $[Mo(CO)_4(5\text{-chloro-}1,10\text{-phen})]$ and $[Mo(CO)_4(4,4'\text{-}Me_2\text{-bpy})]$ (Figures 7.8 and 7.9) also display clean reversible reduction couples for the ligands and irreversible $Mo^{0/+}$ oxidations. There is an additional irreversible oxidation present in these cyclic voltammograms at +1.4 V. This is the $Mo^{0/+}$ oxidation for $[Mo(CO)_6]$, as reported by Cook and Morse.[99] It can be difficult to remove all of the $[Mo(CO)_6]$ starting material from the final product. $[Mo(CO)_4(DPA)]$, $[Mo(CO)_4(ethylenediamine)]$, and $[Mo(CO)_4(TMEDA)]$ (Figures 7.4, 7.5, and 7.7) also display irreversible $Mo^{0/+1}$ oxidations. The DPA, ethylenediamine, and TMEDA ligands are not easily reduced, and thus are not electrochemically active under our conditions.

Overall, the electrochemical data for these complexes demonstrates the anticipated redox trends. Specifically, the effect of the electron donating and withdrawing substituents on the N-N ligand is observed in both the reduction and oxidation potentials. As the electrochemical data for very few $[Mo(CO)_4(N\text{-}N)]$ systems have been reported in the literature, this investigation offers new insight into the redox properties of N-N complexes. The cyclic voltammetric data provides information concerning the nature and energy of the HOMO and LUMO for these $[Mo(CO)_4(N\text{-}N)]$ complexes.

Figure 7.1. Cyclic Voltammogram of $[Mo(CO)_4(bpy)]$. (CH_3CN with 0.1 M Bu_4NPF_6, Ag/AgCl (0.29 V vs. NHE, 0.44 V vs. $Cp_2Fe^{0/+1}$))

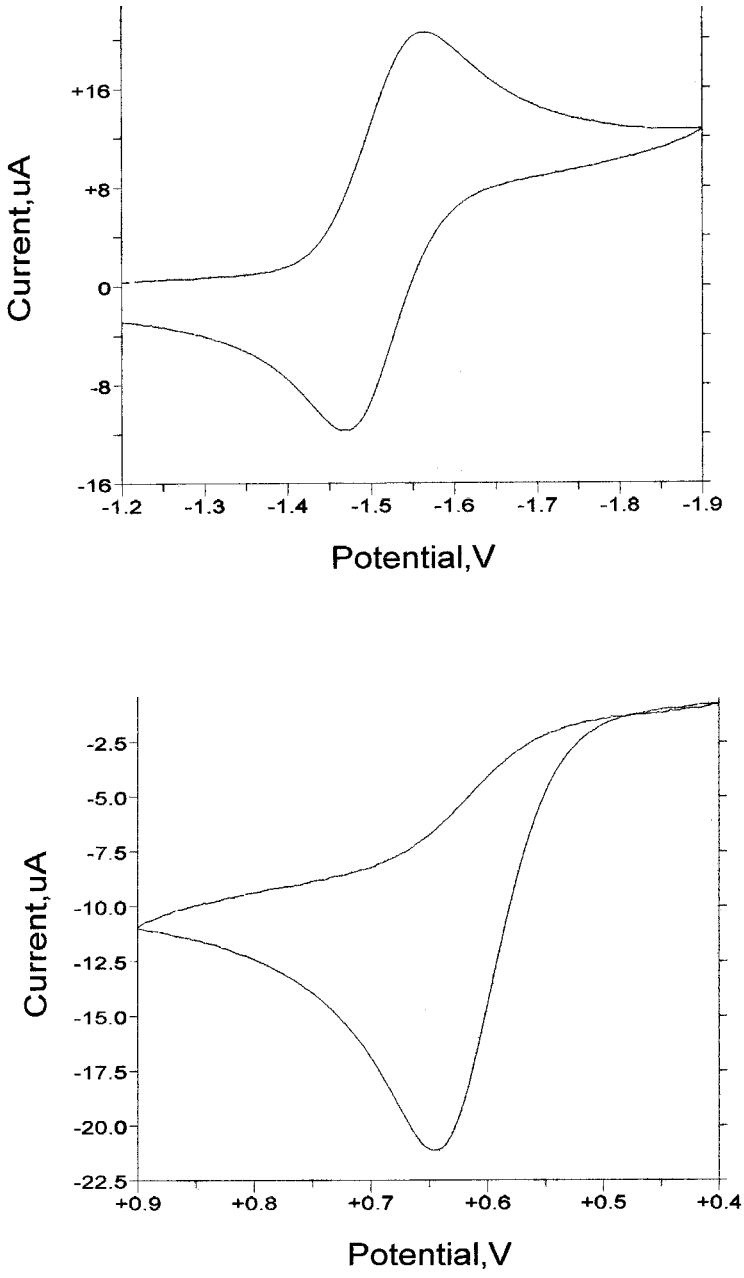

Figure 7.2. Cyclic Voltammogram of [$Mo(CO)_4$(5-nitro-1,10-phen)]. (CH_3CN with 0.1 M Bu_4NPF_6, Ag/AgCl (0.29 V vs. NHE, 0.44 V vs. $Cp_2Fe^{0/+1}$))

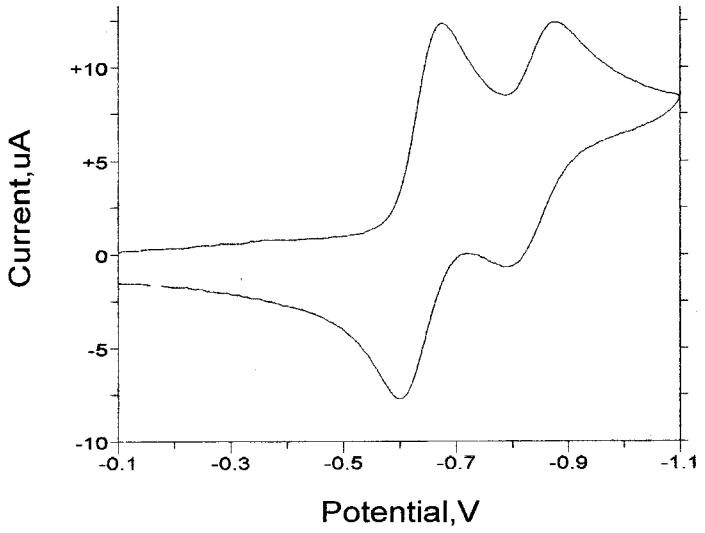

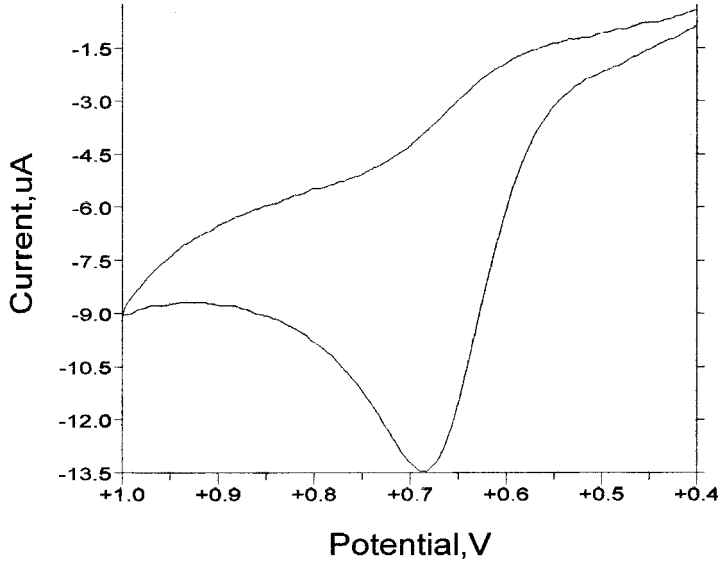

Figure 7.3. Cyclic Voltammogram of $[Mo(CO)_4(1,10\text{-phen})]$. ($CH_3CN$ with 0.1 M Bu_4NPF_6, Ag/AgCl (0.29 V vs. NHE, 0.44 V vs. $Cp_2Fe^{0/+1}$))

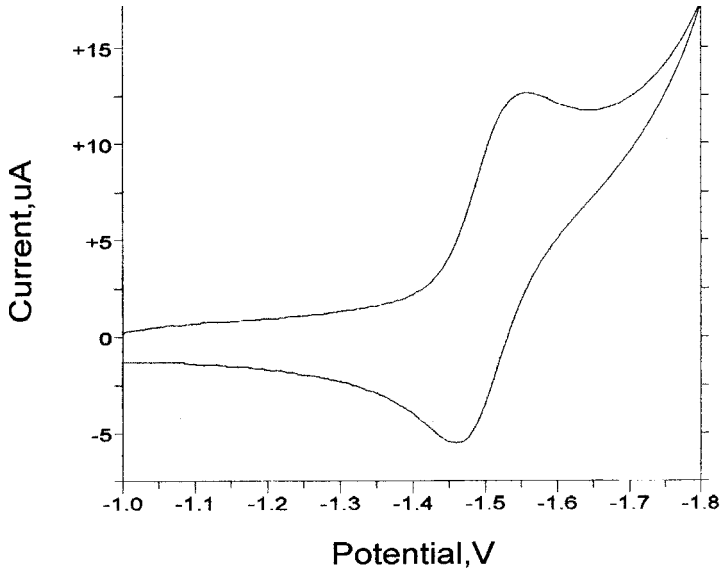

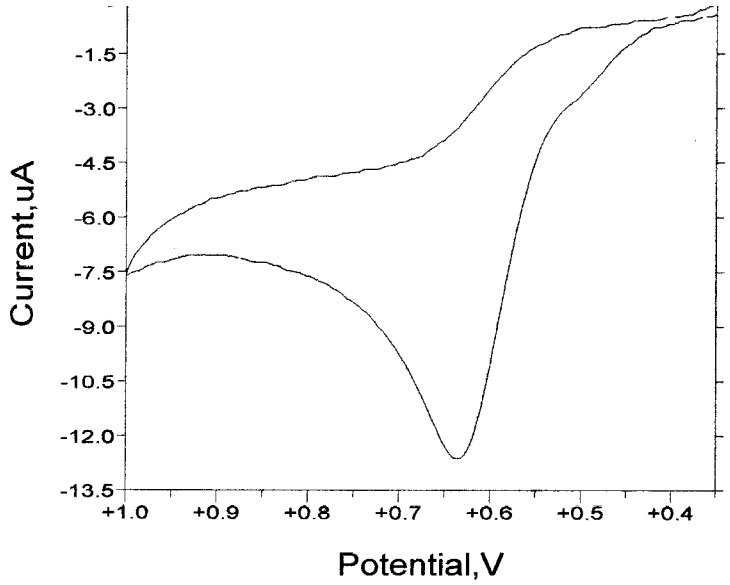

Figure 7.4. Cyclic Voltammogram of [$Mo(CO)_4$(DPA)]. (CH_3CN with 0.1 M Bu_4NPF_6, Ag/AgCl (0.29 V vs. NHE, 0.44 V vs. $Cp_2Fe^{0/+1}$))

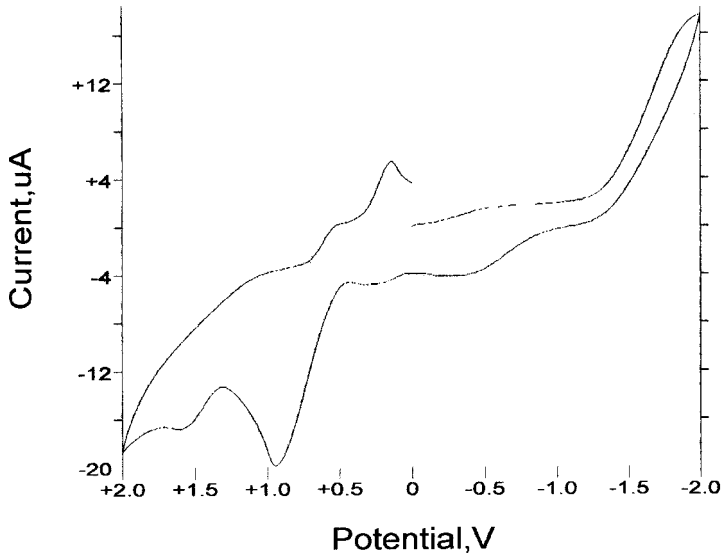

Figure 7.5. Cyclic Voltammogram of [$Mo(CO)_4$(ethylenediamine)]. (CH_3CN with 0.1 M Bu_4NPF_6, Ag/AgCl (0.29 V vs. NHE, 0.44 V vs. $Cp_2Fe^{0/+1}$))

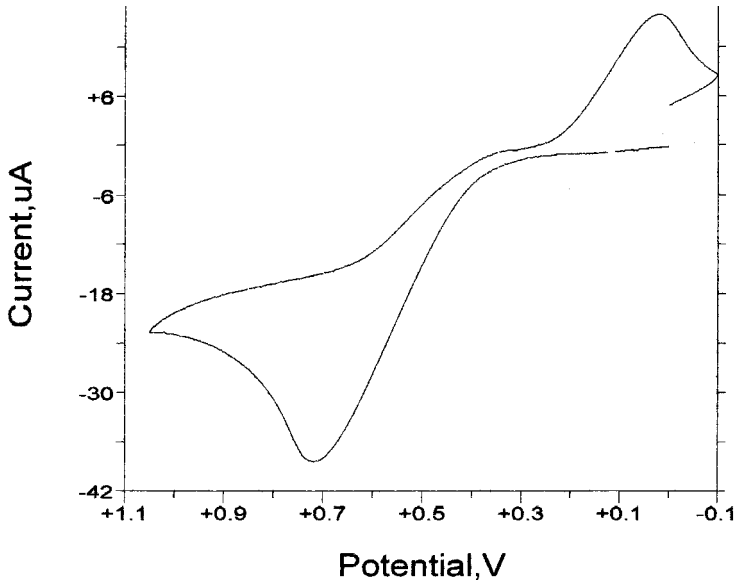

Figure 7.6. Cyclic Voltammogram of [$Mo(CO)_4$(4,7-Ph_2-1,10-phen)]. (CH_3CN with 0.1 M Bu_4NPF_6, Ag/AgCl (0.29 V vs. NHE, 0.44 V vs. $Cp_2Fe^{0/+1}$))

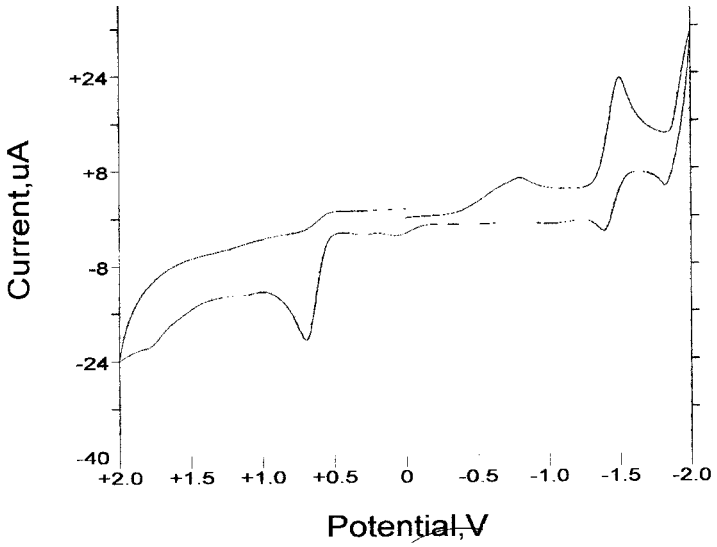

Figure 7.7. Cyclic Voltammogram of [$Mo(CO)_4$(TMEDA)]. (CH_3CN with 0.1 M Bu_4NPF_6, Ag/AgCl (0.29 V vs. NHE, 0.44 V vs. $Cp_2Fe^{0/+1}$))

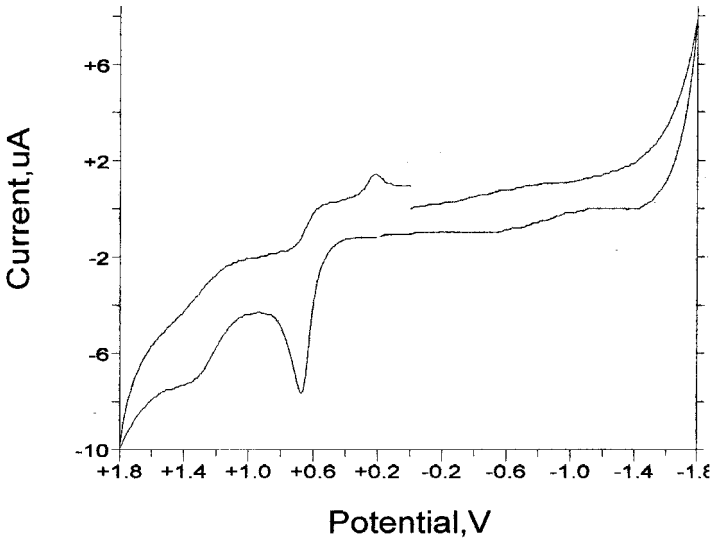

Figure 7.8. Cyclic Voltammogram of $[Mo(CO)_4(4,4'\text{-}Me_2\text{-}bpy)]$. ($CH_3CN$ with 0.1 M Bu_4NPF_6, Ag/AgCl (0.29 V vs. NHE, 0.44 V vs. $Cp_2Fe^{0/+1}$))

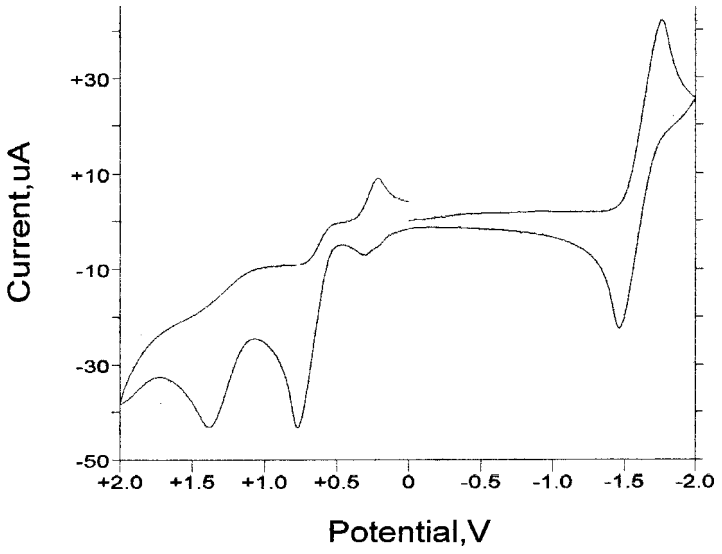

Figure 7.9. Cyclic Voltammogram of $[Mo(CO)_4(5\text{-}Cl\text{-}1,10\text{-}phen)]$. ($CH_3CN$ with 0.1 M Bu_4NPF_6, Ag/AgCl (0.29 V vs. NHE, 0.44 V vs. $Cp_2Fe^{0/+1}$))

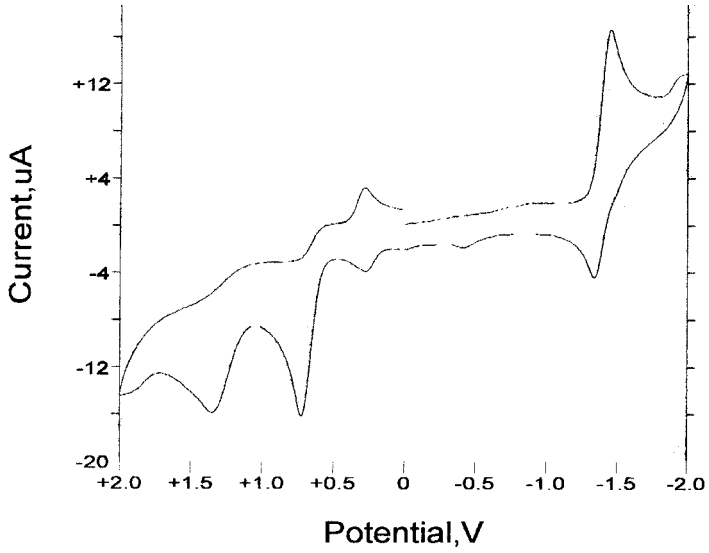

The $[Mo(CO)_4(N\text{-}N)]$ complexes exhibit similar features in their electronic absorption spectra. A summary of the electronic absorption spectral data for the series is shown in Table 7.2. The electronic absorption spectrum for $[Mo(CO)_4(1,10\text{-phen})]$ is shown in Figure 7.10, while the spectra for the remainder of the $[Mo(CO)_4(N\text{-}N)]$ complexes are in Appendices II - X. For this series of $[Mo(CO)_4(N\text{-}N)]$ systems where N-N is a bpy or phen derivative, the electronic absorption spectra consist of $\pi \rightarrow \pi^*$ ligand localized transitions in the ultraviolet region. Metal-to-ligand charge transfer (MLCT) transitions and higher energy absorptions which are $d \rightarrow d$ transitions are found in the visible region, and have been consistently cited in the literature for $[Mo(CO)_4(N\text{-}N)]$ systems.[87-89] The lowest energy transition in the visible region for the bpy and 1,10-phen based systems is the Mo $(d\pi) \rightarrow$ N-N (π^*) metal-to-ligand charge transfer. This MLCT energy varies when the N-N ligand used is varied. The Mo $(d\pi) \rightarrow$ N-N (π^*) CT transition is shifted to lower energy as the π^* energy on the N-N ligand is lowered. The $[Mo(CO)_4(N\text{-}N)]$ complexes that do not have N-N ligands with π systems don't display these π^* or MLCT transitions: N-N = ethylenediamine, DPA, and TMEDA. In these cases, the lowest-lying transition is a $d \rightarrow d$ transition.

Table 7.2. Electronic Absorption Spectroscopy of $[Mo(CO)_4(N\text{-}N)]$ Systems.[a]

N-N	λ_{max}^{abs} (nm)[b]
1,10-phen[c]	482
5-Cl-1,10-phen[d]	498
5-nitro-1,10-phen[d]	520
4,7-Me_2-1,10-phen[d]	407
4,7-Ph_2-1,10-phen[d]	490
bpy[c]	444
DPA	e
en	390[f]
TMEDA	390[f]

[a]Spectra were recorded at room temperature, using acetonitrile. [b]Wavelength of lowest lying transition, Mo $\rightarrow$ N-N CT. [c]Reference 80. [d]Reference 82. [e]No λ_{max}^{abs} detected for this complex. [f]Wavelength of lowest lying transition, not assigned to an MLCT.

Figure 7.10. Electronic Absorption Spectrum for [$Mo(CO)_4$(1,10-phen)] in Acetonitrile at Room Temperature, Glass Cell.

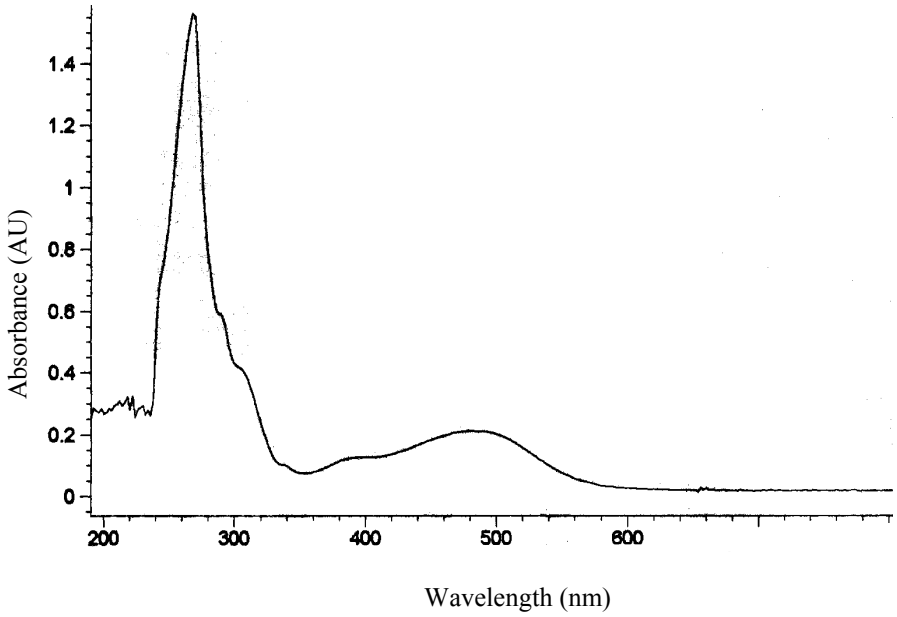

Correlations between the experimentally obtained energy of the lowest lying MLCT, E^{abs}, and the $\Delta E_{1/2}$ for the series of [$Mo(CO)_4$(N-N)] complexes were tested, where $\Delta E_{1/2} = E_p^{a\ oxd} - E_{1/2}^{red}$.[98] The data have been tabulated in Table 7.3; the correlation plot is shown in Figure 7.11. [$Mo(CO)_4$(ethylenediamine)] and [$Mo(CO)_4$(DPA)] do not have ligand-based reductions; therefore these complexes are not included in this correlation. Figure 7.11 shows a poor correlation (R = 0.79) between the lowest lying MLCT and $\Delta E_{1/2}$ for the series of [$Mo(CO)_4$(N-N)] systems tested. Omission of the 5-nitro-1,10-phen complex from the graph significantly improves the relationship, shown in Figure 7.11 (B), but dramatically changes the slope and the intercept. This results in a good linear fit (R = 0.982). This correlation shows a positive relationship between the absorption lowest lying MLCT and the $\Delta E_{1/2}$ for the of [$Mo(CO)_4$(N-N)] systems tested. This finding indicates that the HOMO – LUMO gap, as measured by two experimental techniques correlates well. It should be noted that inclusion of additional

points on the plot, obtained either experimentally or from the literature, could further test this correlation.

Table 7.3. Experimental Lowest Lying MLCT and $\Delta E_{1/2}$ for $[Mo(CO)_4(N\text{-}N)]$ Complexes, where $\Delta E_{1/2} = E_p^{a\ oxd} - E_{1/2}^{red}$.

$[Mo(CO)_4(N\text{-}N)]$ Complex	Expt. E^{abs} (eV)	Expt. $\Delta E_{1/2}$ (eV)
$[Mo(CO)_4(phen)]$	2.57	2.21
$[Mo(CO)_4(5\text{-}Cl\text{-}phen)]$	2.49	2.11
$[Mo(CO)_4(5\text{-}NO_2\text{-}phen)]$	2.39	1.38
$[Mo(CO)_4(4,7\text{-}Ph_2\text{-}phen)]$	2.53	2.13
$[Mo(CO)_4(bpy)]$	2.79	2.35

Electronic absorption spectra and cyclic voltammograms for $[Mo(CO)_4(N\text{-}N)]$ complexes completed in acetonitrile.

Figure 7.11. Experimental Correlation: $\Delta E_{1/2}$ Versus $E_{abs.}$ of the Lowest Lying MLCT for the Series of $[Mo(CO)_4(N\text{-}N)]$ Complexes. N-N ligands used include: 1,10-phen, 5-nitro-1,10-phen, 5-chloro-1,10-phen, 4,7-Ph_2-1,10-phen, and bpy(A). Plot Without 5-nitro-1,10-phen (B).

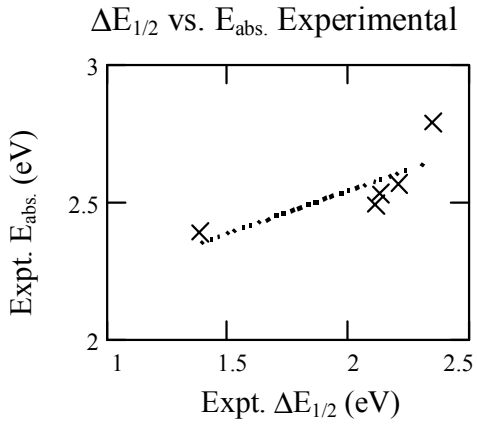

Corr. = 0.792
Slope = 0.31, Intercept = 1.91

A

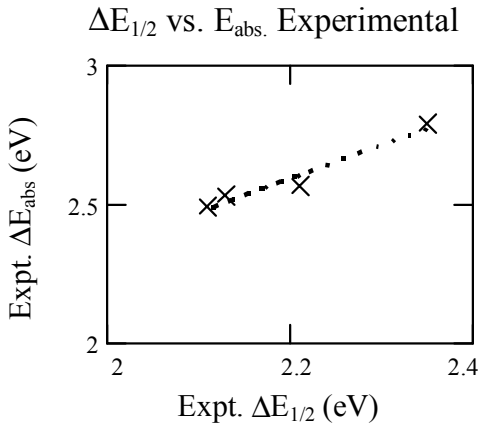

Corr. = 0.982
Slope = 1.21, Intercept = -0.06

B

The $[Mo(CO)_4(N\text{-}N)]$ systems were also characterized by ^1H NMR spectroscopy which is reported in Table 7.4. ^1H NMR spectral investigations of $[Mo(CO)_4(N\text{-}N)]$ systems are not commonly reported in the literature. All NMR spectral measurements were completed in $CDCl_3$ or acetone-d_6 at room temperature. For $[Mo(CO)_4(1,10\text{-phen})]$ and the substituted 1,10-phenanthroline complexes, the assignments are made according to the labeling scheme shown in Figure 7.12. All of the $[Mo(CO)_4(N\text{-}N)]$ systems investigated have sufficiently weak coupling as to allow first-order analyses of the spectra.[97]

Figure 7.12. Labeling Scheme for 1,10-Phenanthroline and Substituted 1,10-Phenanthroline.

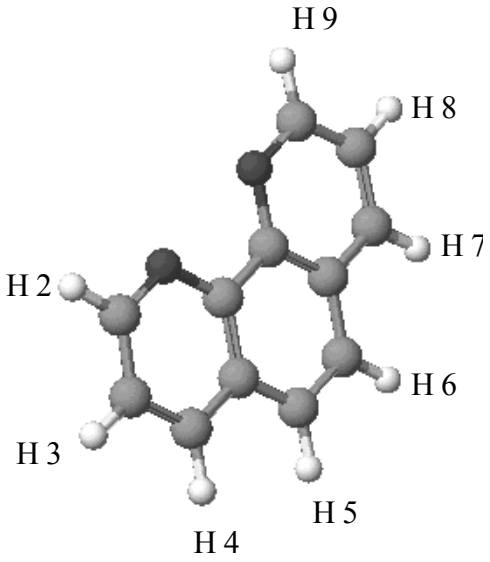

Atom Types: black = nitrogen, gray = carbon, white = hydrogen.

Table 7.4. ^{1}H NMR Chemical Shifts for [$Mo(CO)_4$(N-N)] systems, (δ, ppm).

N-N	Chemical Shift (ppm)	Assignment
1,10-phen[a]	9.48 d (J = 7.9 Hz)	H2
	8.43 d (J = 14.0 Hz)	H4
	7.97 s	H5
	7.75 dd (J = 9.0, 14.0 Hz)	H3
5-Cl-1,10-phen[a]	9.50 dm (1H, J = 5.2 Hz)	H2
	9.42 dm (1H, J = 5.0 Hz)	H9
	8.78 dm (1H, J = 8.6 Hz)	H4
	8.31 dm (1H, J = 7.5 Hz)	H7
	8.03 s	H6
	7.81 dd (1H, J = 8.5, 5.2 Hz)	H3
	7.71 dd (1H, J = 8.2, 5.0 Hz)	H8
5-nitro-1,10-phen[b]	10.13 dd (J = 9.2, 1.3 Hz)	H2
	10.12dd (J = 8.8, 1.3 Hz)	H9
	9.73 dd (J = 8.8, 1.3 Hz)	H4
	9.67 s	H6
	9.55 dd (J = 8.5, 1.3 Hz)	H7
	8.68 dd (J = 10.3, 4.9 Hz)	H4
	8.65 dd (J = 9.7, 5.0 Hz)	H8
4,7-Me_2-	9.12 d (J = 4.2 Hz)	H2
1,10-phen[a]	8.05 s	H5
	7.51 d (J = 3.8 Hz)	H3
	2.82 s	CH_3
4,7-Ph_2-	9.50 d (J = 5.2 Hz)	H2
1,10-phen[a]	7.98 s	H5
	7.66 d (J = 5.2 Hz)	H3
	7.5-7.6 m	C_6H_5
bpy[a]	9.14 d (J = 5.1 Hz)	H2
	8.10 d (J = 8.1 Hz)	H5
	7.94 pt (J = 7.7 Hz)	H4
	7.38 pt (J = 5.6, 6.9 Hz)	H3

Table 7.3. ^{1}H NMR Chemical Shifts for [$Mo(CO)_4$(N-N)] systems, (δ, ppm), Cont.

4,4'-Me_2-bpy[a]	8.92 d (J = 5.5 Hz)	H2
	7.88 s	H5
	7.17 d (J = 5.5 Hz)	H3
	2.51 s	CH_3
DPA	9.58 s (1H, broad)	NH
	8.65 dd (2H, J = 5.7, 1.6 Hz)	H2
	7.87 dpt (2H, J = 7.6, 1.8 Hz)	H4
	7.29 d (2H, J = 8.47)	H5
	7.08 dpt (2H, J = 7, 1.0 Hz)	H3
en[a]		
TMEDA[a]	2.81 s	CH_3
	2.72 s	CH_2

[a] in $CDCl_3$, [b] in acetone-d_6

^{1}H NMR spectra for the [$Mo(CO)_4$(N-N)] complexes are located in Appendices XI – XIX (pp 150 – 158). The proton NMR data for the [$Mo(CO)_4$(1,10-phen)] complex in $CDCl_3$ shows a set of well resolved resonances with chemical shifts ranging from 7.75 to 9.48 ppm. Integration of the spectra yields a 1:1:1:1 ratio of inequivalent protons. Substituted [$Mo(CO)_4$(1,10-phen)] complexes with electron-donating substituents included [$Mo(CO)_4$(4,7-Me_2-1,10-phen)]. Spectra for [$Mo(CO)_4$(4,7-Me_2-1,10-phen)] were recorded in $CDCl_3$. Chemical shifts for this complex ranged from 7.51 to 9.12 ppm. Methyl protons were detected as a singlet at a chemical shift of 2.82 ppm. Chemical shifts for this complex are shifted upfield relative to [$Mo(CO)_4$(1,10-phen)] due to the substitution of the methyl groups at the 4 and 7 positions. This addition of electron density causes shielding of the neighboring protons. Substituted [$Mo(CO)_4$(1,10-phen)] complexes with electron-withdrawing substituents included [$Mo(CO)_4$(5-Cl-1,10-phen)], [$Mo(CO)_4$(5-nitro-1,10-phen)], and [$Mo(CO)_4$(4,7-Ph_2-1,10-phen)]. The ^{1}H NMR data

for all three complexes were recorded in $CDCl_3$. These spectra show sets of well resolved resonances with chemical shifts ranging from 7.71 to 9.50 ppm for $[Mo(CO)_4(5\text{-}Cl\text{-}1,10\text{-}phen)]$, and 7.66 to 9.50 ppm for $[Mo(CO)_4(4,7\text{-}Ph_2\text{-}1,10\text{-}phen)]$. For the latter complex, the phenyl protons were detected as a multiplet at a chemical shift of 7.50 to 7.60 ppm. The 5-Cl-1,10-phen complex's resonances all integrated for a 1:1 ratio of inequivalent protons. ^1H NMR data for the 5-nitro complex shows a set of well-resolved resonances with chemical shifts ranging from 8.68 to 10.13 ppm, all resonances integrated for a 1:1 ratio of inequivalent protons. Chemical shifts for these complexes are shifted downfield relative to $[Mo(CO)_4(1,10\text{-}phen)]$ due to the presence of electron-withdrawing groups. ^1H NMR spectra were also obtained for $[Mo(CO)_4(bpy)]$ and $[Mo(CO)_4(4,4'\text{-}Me_2\text{-}bpy)]$ in $CDCl_3$. The bpy complex displayed resonances with chemical shifts ranging from 7.38 to 9.14 ppm. Resonances for the methyl substituted complex were shifted upfield, chemical shifts ranging from 7.17 to 8.92 ppm. Methyl protons were detected as a singlet at a chemical shift of 2.51 ppm. The spectrum for the bpy complex integrated for a 1:1:1:1 ratio of inequivalent protons, the 4,4'-Me_2-bpy complex integrated for a 1:1:1:3 ratio of inequivalent protons. $[Mo(CO)_4(DPA)]$ displayed resonances with chemical shifts ranging from 7.08 to 9.58 ppm in the proton spectrum. The broad singlet at 9.58 ppm was due to the amine proton. Remaining resonances (7.08 to 8.65 ppm) are shifted upfield as compared to the spectrum for $[Mo(CO)_4(bpy)]$ due to the electron donating effect of the amine group. The ^1H NMR spectrum for $[Mo(CO)_4(TMEDA)]$ in $CDCl_3$ consisted of two singlets, with chemical shifts at 2.72 and 2.81 ppm.

The spectra for the series of $[Mo(CO)_4(N\text{-}N)]$ complexes are consistent with the structures of the molecules. ^1H NMR spectra provides valuable information about the $[Mo(CO)_4(N\text{-}N)]$ complexes. The effect of substituting electron donating or withdrawing groups on the N-N ligand is reflected in the chemical shift.